# Semi-Automated Method for Quantifying and Localizing White Matter Hyperintensities on MR Images

M. Wu[1], C. Rosano[2], M. Butters[3], E. Whyte[3], R. Crooks[2], C. C. Meltzer[4], C. F. Reynolds III[3], H. J. Aizenstein[3]

[1]Department of Electrical & Computer Engineering, University of Pittsburgh, Pittsburgh, PA, United States, [2]Epidemiology, University of Pittsburgh, Pittsburgh, PA, United States, [3]Psychiatry, University of Pittsburgh, Pittsburgh, PA, United States, [4]Radiology, University of Pittsburgh, Pittsburgh, PA, United States

## Introduction

A number of previous studies have shown that white matter hyperintensities (WMH) are associated with neuropsychiatric disorders, including vascular dementia [1], Alzheimer's disease [2], and late-onset late-life depression (LLD) [3]. These studies have primarily used a semi-quantitative rating system, in which trained expert raters visually grade the WMH using 4-point or 10-point scales. This method requires personal judgment, and it does not convey accurate information about the location or the volume of WMHs. A number of automatic or semi-automatic methods have been implemented for WMH segmentation in FLAIR images. In these methods, a lower intensity threshold is usually chosen for WMH segmentation, such as using 3.5 standard deviations of the intensity value of the normal WM [4]. To exclude the misclassified non-WMH voxels, Hirono [4] uses a manually outlined mask of WHMs with surrounding WM, GM and CSF, while Wen [5] uses a WM probability map (MNI 152 brains) to favor the most likely WM regions. Manually outlining the WMH mask [4] is labor-intensive, while the method used by Wen [5] makes WM segmentation accuracies rely on MNI to subject registration accuracies.

## Methods

In the current study, we present an alternative method for WMH quantification and localization, which uses a fuzzy connected algorithm [6] to segment the WMHs and the Automated Labeling Pathway (ALP) to localize the WMHs into the anatomical space. This WMH segmentation method allows the user to choose multiple seeds from the scattered WMH clusters in a 3D FLAIR brain image (implemented in C++ using Fast Light ToolKit (FLTK), Insight Segmentation and Registration Toolkit (ITK))[7]. For each seed, the fuzzy connected algorithm uses different parameters to form a WMH cluster (containing the respective seed), and the system combines the scattered WMH clusters into the final WMH segmentation. This method avoids using a single cut-off threshold for the whole brain or a single slice of brain and potentially offers more precise WMH segmentation. Unlike in Hirono's method [4], this semi-automatic method only involves WMH seed selection, which requires only a small amount of manual interaction. ALP is used (Fig. 1) to accurately localize the WMHs. This is an automated method we developed to automatically label specific anatomic regions of interest. In the current study, the standard Montreal Neurological Institute (MNI) brain Colin27, which carries high anatomical details and has a high spatial resolution (1mm$^3$ voxel size), was used as the template; the 14 lobar regions and hemispheres identified in the Talairach Deaemon were chosen as anatomical atlas.

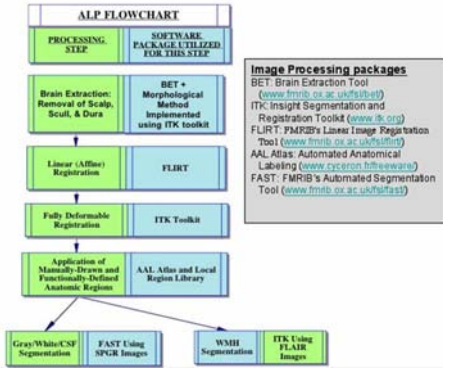


Fig. 1. ALP Flowchart.

Ten patient subjects (4 male; mean age 72.2, standard deviation ±5.57; all having LLD; mean Hamilton Depression Rating Scale19.8, standard deviation ± 6.18) were scanned using a 1.5 Tesla Signa Scanner (GE Medical Systems, Milwaukee, WI). 3D structural MR images were acquired at sagittal orientation using 3D SPGR (TR/TE = 25/5 ms; flip angle = 40º; FOV = 24×18cm, slice thickness = 1.5mm, matrix size = 256×192). And fast fluid-attenuated inversion recovery (fast FLAIR) images were acquired at axial orientation (TR/TE = 9002/56 ms Ef; TI = 2200 ms; NEX = 1; FOV = 24 cm; slice thickness = 5 mm; slice gap = 1 mm; matrix size = 192×256). A numerical rating for WMH was assigned by comparison of each subject's imaging data to predefined visual standards using a 10-point scale. For each FLAIR scan WMH ratings were made by two independent raters. If the ratings differed by one point, the final rating was the mean of the two values. A difference greater than one point between raters was considered as a disagreement, and was adjudicated by consensus.

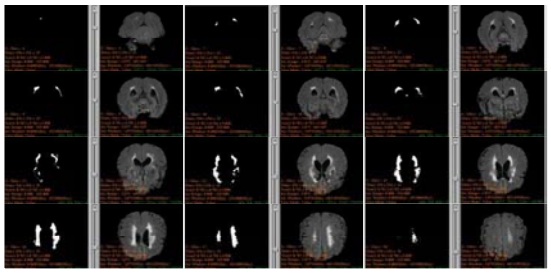

Fig. 2. Twelve pairs of segmented WMHs versus FLAIR slices from one subject are shown. Left slice is the WMH result; right one is the associated FLAIR slice.

## Results

**WMH segmentation Evaluation**: The WMH segmentation results of 10 subjects using this semi-automated method were statistically significant compared to the manual grading of WMH visual ratings. The comparison was done both with a linear regression model and the correlation coefficient. The normalized automated WMH segmentation results were found to be significantly correlated to the visual grades with a high R-squared = 0.822, F(1,9) = 37.0, p = 0.0003, and a high correlation coefficient at 0.907. The high correlation between the semi-automated results and the visual grades demonstrates that this semi-automated method can segment the WMHs successfully. The WMH segmentation result of one subject is displayed in Fig. 2, showing this method's effective segmentation of WMHs.

**Localization of WMHs**: Using ALP, the atlas in the MNI template Colin27 was transferred to the subject's 3D SPGR image and further into the subject FLAIR image space, which were used as ROI masks to localize the WMHs. These WMH volume estimates describe the spatial distribution of the WMH burden. From the table, we can see the WMHs occur primarily in the subcortical, frontal, and temporal areas. This is consistent with the observations in the literature of these areas being prominently affected in LLD. It should be noted in the table that there is considerable variability across subjects in the locations of the WMHs. For instance, half of the subjects have more WMH burden in the frontal versus temporal lobes and the other half have more WMH burden in the temporal lobe versus the frontal lobe. These differences raise the possibility that the locations of WMH burden could explain some of the variability in patients' characteristics and treatment response.

**Table 1:** Volumes of WMH (mm$^3$) per region for the ten subjects

| Reg\Sub | 1 | 2 | 3 | 4 | 5 | 6 | 7 | 8 | 9 | 10 |
|---|---|---|---|---|---|---|---|---|---|---|
| cerebellum ant/post | 0 | 0 | 0 | 0 | 0 | 0 | 0 | 0 | 0 | 0 |
| frontal | 2778 | 4 | 617 | 1026 | 387 | 1445 | 4771 | 12578 | 953 | 390 |
| limbic | 748 | 0 | 548 | 197 | 77 | 577 | 3460 | 4402 | 117 | 44 |
| medulla | 0 | 0 | 0 | 0 | 0 | 0 | 0 | 0 | 0 | 0 |
| midbrain | 0 | 0 | 0 | 0 | 0 | 0 | 0 | 0 | 0 | 0 |
| occipital | 2336 | 1982 | 861 | 2931 | 2599 | 1916 | 850 | 617 | 0 | 934 |
| parietal | 416 | 0 | 11 | 33 | 73 | 456 | 767 | 3602 | 478 | 0 |
| pons | 0 | 0 | 0 | 0 | 0 | 0 | 0 | 0 | 0 | 0 |
| subcortical | 5785 | 197 | 11556 | 5077 | 2573 | 4201 | 26546 | 31689 | 1653 | 1825 |
| temporal | 3734 | 124 | 1372 | 2150 | 584 | 1332 | 3011 | 9614 | 350 | 142 |
| left mask | 5282 | 1566 | 11621 | 5599 | 3216 | 2781 | 19465 | 32127 | 2716 | 1683 |
| right mask | 10654 | 807 | 7424 | 6238 | 3165 | 7384 | 20192 | 30266 | 847 | 2018 |

## Conclusion

Quantification and localization of WMHs is critical for research in the risk factors and pathogenesis of neuropsychiatric disorders. Most methods previously used were labor intensive, subjective, and provided little if any anatomic localization. The current method solves many of the previous limitations: it requires only a small amount of manual intervention, provides WMH volume estimates, and localizes the WMH burden to a number of anatomic ROIs, which will facilitate further, fine-grained understanding of the role of WMH in pathogenesis of neuropsychiatric disorders.

## References

[1] van Gijn J. Neurol 1998; 51:S3-8. [2] Mirsen T. et al. Arch Neurol 1991; 48:1015-1021. [3] Alan J. et al. J Affective Disorders 2004; 79(1-3):81-95. [4] Hirono N. et al. Stroke 2000; 31:2182 – 2188. [5] Wen W. et al.Neuroimage 2004; 22(1):144-54. [6] Udupa JK et al. IEEE Trans Med Imaging 1997;16(5):598-609. [7] www.fltk.org, www.itk.org.